Thermochimica Acta 520 (2011) 110–120

Contents lists available at ScienceDirect

Thermochimica Acta

journal homepage: www.elsevier.com/locate/tca

Eucalyptus kraft pulp production: Thermogravimetry monitoring

Agustín G. Barneto[a,*], Carlos Vila[b], José Ariza[a]

[a] Chemical Engineering Department, Campus El Carmen, University of Huelva, 21071 Huelva, Spain
[b] Department of Textile and Paper Engineering, Universitat Politècnica de Catalunya, Colom 11, E-08222 Terrassa, Spain

ARTICLE INFO

Article history:
Received 19 January 2011
Received in revised form 22 March 2011
Accepted 26 March 2011
Available online 4 April 2011

Keywords:
Eucalyptus
Wood
Pulp
Thermogravimetry
Modeling

ABSTRACT

Under oxidative environment the thermal degradation of lignocellulosic materials like wood or pulp is sensitive to slight composition changes. For this, in order to complement the chemical and X-ray diffraction results, thermogravimetric analyses (TGA) were used to monitor pulp production in a modern pulp mill. Runs were carried out on crude, oxygen delignified and bleached pulps from three eucalyptus woods from different species and geographical origins. Moreover, with the modeling of thermogravimetric data, it was possible to obtain an approximate composition of samples which includes crystalline and amorphous cellulose. TGA results show that pulping has an intensive effect on bulk lignin and hemicellulose, but it has limited influence on the removal of these substances when they are linked to cellulose microfibril. The stages of oxygen delignification and bleaching, based in chlorine dioxide and hydrogen peroxide, increase the crystalline cellulose volatilization rate. These changes are compatible with a more crystalline microfibril. The influence of the fibre size on pulp composition, crystallinity and thermal degradation behavior was observed.

1. Introduction

It is known that, in the wood cell wall, cellulose chains are bonded in a parallel way yielding microfibrils which usually have an equatorial dimension between 2 and 6 nm. In higher plants the cellulose microfibril is a thin and long crystalline structure which contains crystalline and amorphous regions [1]. Crystalline cellulose forms crystallites along the microfibril but amorphous cellulose maybe found between crystallites along the microfibril or in the microfibril surface [2]. Native cellulose (cellulose I) is present as two allomorphs: Iα (triclinic) and Iβ (monoclinic). Iβ is present in greater proportion in higher plants. As for cellulose microfibril bundles, they form larger structures known as microfibril aggregates with an equatorial dimension of 20–30 nm. Microfibril aggregates are embedded in a matrix which contains hemicellulose, lignin and other substances like pectin and proteins [3]. Thus, in microfibril aggregates there are accessible and inaccessible microfibril surfaces. This fact has been tested using solid-state cross-polarization magic angle spinning carbon-13 nuclear magnetic resonance (CP/MAS ^{13}C NMR) spectroscopy [4]. The specific role of microfibril surface has been pointed by computational model, which shows that the structure of the microfibril surface is qualitatively different to the crystalline interior because the hydrogen bonding organization is altered [5].

According to recent statistics [6] eucalyptus wood mean values are close to 10% of the whole wood consumption in CEPI countries (Confederation of European Paper Industries). However, softwoods as spruce (38.6%) or pine (31.5%) are the most used wood species in pulp-paper industry in Europe. The chemical pulping based on the kraft process is the worldwide dominating technology for liberating the fibers from wood. The chemical core of the typical kraft pulping process is the digester, a cooking vessel where wood chips are in contact with white liquor, an aqueous solution of sodium sulphide and sodium hydroxide. The white liquor dissolves lignin, producing a pulp from fibrous carbohydrates (mainly cellulose) present in wood. After it is taken out of the digester, the pulp is soaked in black liquor, involving a necessary and intensive washing in order to obtain crude pulp. Next, in a modern pulp mill, oxygen delignification and bleaching processes based on chlorine dioxide and hydrogen peroxide are usually applied.

The delignification process includes several reaction types (i.e. cleavage of aryl ether bonds) which produce soluble and low molecular weight fragments from the tridimensional network of lignin. At the same time, both hemicellulose and cellulose undergo degradation which diminishes the pulping yield. Under alkaline conditions, the amorphous hemicellulose is easily hydrolyzed, undergoing peeling and chain-termination reactions. Cellulose, which contains crystalline and amorphous zones, is subjected to the same reactions, producing a decrease in pulp viscosity [7]. In order to improve kraft pulping, several methods have been proposed. Some have pointed out the importance of controlling the alkalinity and caustic-

* Corresponding author. Tel.: +34 959 219982; fax: +34 959 219983.
E-mail address: agustin.garcia@diq.uhu.es (A.G. Barneto).

0040-6031/$ – see front matter © 2011 Elsevier B.V. All rights reserved.
doi:10.1016/j.tca.2011.03.027

ity in the digester [8,9], and others the importance of using additives like antraquinone to avoid cellulose degradation [10].

In a thermogravimetric analysis (TGA) a small sample is subjected to a heating program under a controlled atmosphere, usually nitrogen (inert) or air (oxidative). During heating, the sample undergoes a progressive degradation process which produces mass losses that are measured using a sensitive balance. For lignocellulosic materials like wood or pulp, the thermal degradation profile (DTG curve, obtained by representing mass loss rate versus temperature) has a characteristic shape. In both inert and oxidative atmospheres, degradation starts between 150 °C and 200 °C producing the cellulose volatilization between 300 °C and 350 °C. Previously, at lower temperature, hemicellulose volatilized causing a particular shoulder in DTG curve close to 250 °C. Lignin degrades in a broad temperature interval, reaching more than 400 °C in inert atmosphere [11,12]. Under this environment, at high temperatures, mass losses from char volatilization are significant [13,14]. If TGA runs are performed with air, the cellulosic volatilization peak is accompanied by another peak at 450 °C. This peak is the consequence of char oxidation [15]. In order to study the thermal behavior of individual components of lignocellulosic materials, the thermogravimetric data has been recently fitted from a kinetic model based on the nucleation concept [13]. The data obtained allows calculating the sample composition and the cellulose crystallinity.

In an industrial process, the pulp is characterized using standardized analysis like kappa number, brightness or viscosity. These analyses give little information about changes that cellulosic fibers undergo. For it, in order to complement this information, in the present work thermogravimetric analysis and X-ray diffraction have been used to study the characteristics of three eucalyptus woods and their pulps obtained along the delignification and bleaching process in a pulp mill. The main objective of this study is to compare the thermal degradation profile of samples to assess the efficiency of pulp production.

2. Materials and methods

2.1. Samples

Samples of *Eucalyptus Grandis* from Uruguay (EGrU), *Eucalyptus Globulus* from Chile (EGlC), and *E. Globulus* from Spain (EGlS) were obtained from ENCE plantations (ENCE is Empresa Nacional de Celulosas de España, a company dedicated to the forestry resources plantation and its processing into pulp and renewable energy). Pulps were obtained from EGrU wood in the ENCE mill at Huelva (Spain) after the following stages: washing of the crude pulp, oxygen delignification, first chlorine dioxide treatment, peroxide treatment, and second chlorine dioxide treatment. These pulps were denominated as: E2, E3, E4, E5 and E6, respectively.

2.2. Kappa number, brightness and viscosity

Kappa number was determined by Tappi T-236. Brightness was measured by ISO 3688. Viscosity was measured by ISO 5251/1.

2.3. Pulp fibre fractionation

A laboratory Bauer–MacNett classifier with screen sizes of 30, 50 and 200 mesh was used to separate pulp fibers according to TAPPI T233-cm-06. For fibre separation, 10 g of pulp were disintegrated in 3000 mL of water and poured into the first chamber. A continuous flow of water passes through this chamber. The pulp, carried by the water flow, is consecutively collected in the screens. The fraction passing through the screen with the 200 mesh sieve was considered as fines. After 20 min of operation the flow of water was stopped and the three fractions were recovered and the content of each one was determined.

2.4. High pressure liquid chromatography (HPLC)

Aliquots of raw material were subjected to moisture, extractives determination (TAPPI T-264-om-88) and to quantitative acid hydrolysis [16]. The solid residue after hydrolysis was recovered by filtration and the content was measured gravimetrically and considered as klason lignin. The high-performance liquid chromatography (HPLC) analysis of liquors from quantitative acid hydrolysis allowed the determination of their contents of monosaccharides from cellulose and hemicellulose. Chromatographic determination was performed using an Agilent 1100 HPLC equipped with an ion-exchange resin Aminex HPX-87H column under the following conditions: mobile phase, 0.006 mol/L of sulfuric acid; flow rate, 0.6 mL/min; and column temperature, 60 °C. As mannose, xylose and galactose were co-eluted in chromatograms, additional analyses were carried out after neutralization of the samples with $BaCO_3$ using an ion-exchange column Aminex HPX-87P. The Aminex HPX-87P column was maintained at 80 °C, and the sugars were eluted with Milli-Q filtered water at a flow rate of 0.6 mL/min. The quantitative acid hydrolysis was made in duplicate and the mean value was used in the statistical calculations.

2.5. Thermogravimetric analysis

TG runs were carried out with a Mettler Toledo model TGA/SDTA851e/LF1600 on samples of around 5 mg under nitrogen and synthetic air (N_2:O_2 4:1) environments, using three heating rates (5, 10, and 20 °C/min) from 25 °C to 900 °C.

In order to obtain the individual degradation behavior of the main components in the studied samples, thermogravimetric data were fitted from wood and pulp simplified models based on pseudo-components (a fraction of sample, not necessarily a pure substance, which thermally degrades in a specific way into a specific temperature interval) [13,14]. Five pseudo-components which represent hemicellulose (H), crystalline cellulose (C_1), amorphous cellulose (C_2), lignin (L) and extractives (E) were used for wood. However, for pulp, only the first four were used, because extractives presence in pulp was assumed as residual. In the present approximation it is accepted that under inert atmosphere solid pseudo-components (S_i) undergo volatilization that yield light volatiles (V_{i1}) and char (R_i), which remains in thermobalance. Under air environment, this char previously obtained, oxidizes yielding new volatiles (V_{i2}) (see Fig. 1). Kinetic parameters for pseudo-components degradation have been obtained from literature or previous studies [12–15,17–28]. The pseudo-components volatilization has been simulated using a nucleation model based on the Prout–Tompkins equation (Eq. (1)) [29–31], where α represents the reaction conversion, k the kinetic constant (expressed according to the Arrhenius law: $k = k_1^0 \exp((-E)/RT)$), where k_0 is the pre-exponential factor and E de activation energy, n the reaction order, m the nucleation order, and s a constant (assumed as 0.01) that ensures reliable values for the reaction rate when reaction conversion is close to extreme values (0 and 1).

$$\frac{d\alpha}{dt} = k(1-\alpha)^n(s+\alpha^m) \quad (1)$$

The pre-exponential factor (k_0) and the activation energy (E) are mainly related with the position of the maximum of DTG curve. The reaction order (n) and the nucleation order (m) basically control the shape of the curve: increasing n or diminishing m results in a broader curve. However, these basic tendencies are merged. For example, increasing m DTG curve appears sharper but also displaces it to higher temperature. The integration and optimization

a

$$S_H \xrightarrow{1} V_{H1} + R_H$$
$$S_{C_1} \xrightarrow{2} V_{C_1 1} + R_{C_1}$$
$$S_{C_2} \xrightarrow{3} V_{C_2 1} + R_{C_2}$$
$$S_L \xrightarrow{4} V_{L1} + R_L$$
$$S_E \xrightarrow{5} V_{E1} + R_E$$

b

$$S_H \xrightarrow{1} V_{H1} + R_H$$
$$R_H \xrightarrow{2} V_{H2}$$
$$S_{C_1} \xrightarrow{3} V_{C_1 1} + R_{C_1}$$
$$R_{C_1} \xrightarrow{4} V_{C_1 2}$$
$$S_{C_2} \xrightarrow{5} V_{C_2 1} + R_{C_2}$$
$$R_{C_2} \xrightarrow{6} V_{C_2 2}$$
$$S_L \xrightarrow{7} V_{L1}$$
$$S_L \longrightarrow R_L \xrightarrow{8} V_{L2}$$
$$S_E \xrightarrow{9} V_{E1} + R_E$$
$$R_E \xrightarrow{10} V_{E2}$$

Fig. 1. Thermal degradation models for wood pyrolysis (a), and wood combustion (b).

of the kinetic equations were carried out using the Runge–Kutta and Gauss–Newton methods, respectively.

2.6. X-ray diffraction

XRD measurements were performed with Cu $K\alpha_1$ radiation ($\lambda = 0.15418$ nm) at 40 kV and 30 mA using a SIEMENS D-500 BRAG-BRENTANO $\theta/2\theta$ geometry X-ray diffractometer. A divergence aperture of 0.3° and a reception aperture of 0.05° were used. Sweeps of 5° to 5° 2θ were made with a step size of 0.05° and step time measurement of 10 s.

The experimental XRD signal was fitted by the use of gaussian distributions, which include amorphous background. The crystallinity of pulps was obtained as the ratio between the area of the crystalline cellulose peaks and the total area, which includes the amorphous background contribution [32].

The equatorial dimension of the crystallites was determined by using (2,0,0) reflection. The full width at half maximum (FWHM) of the diffraction peaks was used to determine crystallite width B_{hkl} by using the Scherrer equation:

$$B_{hkl} = \frac{0.9\lambda}{\sqrt{(\Delta 2\theta)^2 - (\Delta 2\theta_0)^2}\cos\theta}$$

where λ is the X-ray wavelength, $\Delta 2\theta$ is the FWHM of each peak, $\Delta 2\theta_0$ is the apparatus broadening and θ the Bragg angle.

3. Results and discussion

In a kraft pulp mill the raw pulp is produced in a batch digester system (see Fig. 2). After wood chips and chemicals are loaded into the digester, cooking is operated according to the following phases: (i) increasing temperature to reach 165 °C (60–75 min), (ii) digestion at 165 °C and 8 atm pressure (50–60 min), (iii) unload (15–20 min). Usually, the factor H (product of the temperature in degree Celsius and the time in hour) is between 400 and 475 °Ch. According to the facility design, for *E. Globulus* these operative conditions assure a yield of the wood pulping process between 53 and 57%, yielding a crude pulp with a kappa index of 15–20 and a viscosity of 1000–1200 mL/g.

At the digester exit, the raw pulp is impregnated in black liquor and contains uncooked wood. Then, it is pumped to the knotting system and the screen room. Accepts from knotters feed the screen room. The screen room consists of three stages (primary, secondary and vibratory screens) which operate in cascade. Rejects from both the knotting system and the screen room are sent back to the digesters. At the end of this separation stage, the black liquor is removed and the pulp is washed, showing a whitish color (E2, crude pulp).

Table 1
Eucalyptus woods compositions obtained by HPLC analysis (average value and standard deviation) (dry basis).

	E. Grandis Uruguay (g/100 g)	*E. Globulus* Chile (g/100 g)	*E. Globulus* Spain (g/100 g)
Glucan	43.5 ± 0.5	47.4 ± 0.5	43.58 ± 0.02
Xylan	11.9 ± 0.5	14.2 ± 0.1	15.36 ± 0.03
Arabinan	0.24 ± 0.01	0.23 ± 0.04	0.32 ± 0.01
Galacturonic acid	0.9 ± 0.2	0.77 ± 0.01	0.94 ± 0.03
Glucuronic acid	1.5 ± 0.2	1.33 ± 0.01	1.45 ± 0.01
Ramnanose	0.30 ± 0.01	0.34 ± 0.04	0.33 ± 0.01
Acetyl group	3.1 ± 0.1	3.32 ± 0.01	3.6 ± 0.2
Klason lignin	31.2 ± 0.3	24.5 ± 0.1	26.1 ± 0.3
Extractives	5.1 ± 0.6	5.9 ± 0.4	5.0 ± 0.5

In an elemental chlorine free bleaching, the crude pulp, previously oxygen delignified, is mainly treated with chlorine dioxide and hydrogen peroxide according to different sequences. In the studied pulp mill the bleaching sequence is D–P–D (chlorine dioxide–peroxide–chlorine dioxide). Oxygen delignification is developed in a tubular reactor according to the following conditions: 15% consistency (solid content of pulp), 15 kgO_2/tonAD (tonAD is tons of air dried pulp, approximately with 10% moisture), pH 11. The first chlorine dioxide treatment: 10% consistency, 37 kg ClO_2/tonAD, pH 5. The hydrogen peroxide treatment: 10% consistency, 4.5 kg H_2O_2/tonAD, 7 kg O_2/tonAD, pH 11. The second chlorine dioxide treatment: 10% consistency, 4 kg ClO_2/tonAD, pH 5.

3.1. Eucalyptus wood characterization

3.1.1. Chemical and X-ray diffraction analysis

Table 1 shows the composition of three eucalyptus woods on the basis of the main sugar monomers detected by HPLC. As it can be seen, among the analyzed woods, the *EGlC* has the highest content in glucan (47.4 wt%) and the lowest in klason lignin (24.5 wt%). On the opposite, *EGrU* has the lowest content in glucan (43.5 wt%) and the highest in klason lignin (31.2 wt%). *EGlS* has an intermediate position, showing the highest hemicellulose content. Extraction in benzene–ethanol shows that the extractives content ranges between 5 and 6 wt%. As it was expected from cellulose contents, X-ray diffraction shows that *EGlC* and *EGrU* have the highest and lowest crystallinity (35.4% and 31.2%), respectively. In all cases the equatorial dimension of the cellulosic microfibril has similar values, ranging between 2.1 and 2.2 nm (see Table 2).

Table 2
Crystallinity and equatorial dimensions of microfibrils in three eucalyptus woods and their respective crude pulps.

	Crystallinity XRD (%)	Equatorial dimension B_{200} (nm)
EGrU wood	31.2	2.1
EGlS wood	33.4	2.2
EGlC wood	35.4	2.2
Crude pulp from EGrU	57.1	3.7
Crude pulp from EGlS	60.4	4.0
Crude pulp from EGlC	62.5	4.1

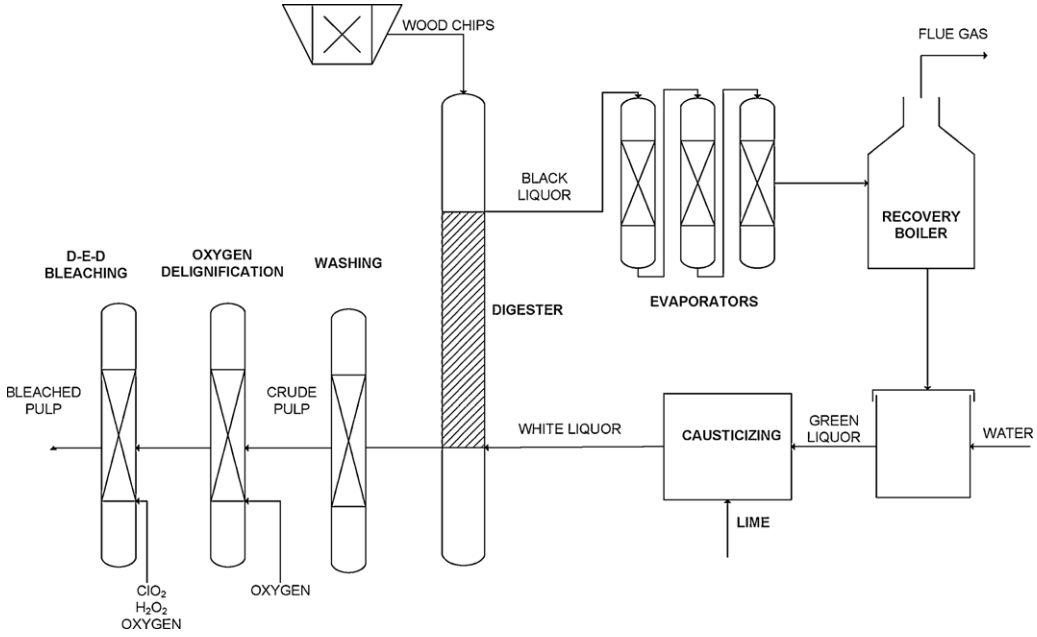

Fig. 2. Kraft pulp mill scheme.

3.1.2. Thermal degradation of eucalyptus woods

Thermogravimetric analysis shows that eucalyptus wood has a characteristic degradation path (see Fig. 3). Usually, the thermal degradation profiles of the lignocellulosic materials (i.e. woods or pulps) are interpreted as the addition of the independent degradations of their main components: hemicellulose, cellulose and lignin. Under inert and oxidative environments, the cellulose volatilization causes the main peak in the DTG curve. Hemicellulose volatilizes at a lower temperature compared with cellulose, producing in both environments a significant shoulder. Finally, lignin is the most resistant component to volatilization, producing a broad tail during pyrolysis that extends to high temperatures. Recently, this standard interpretation of pyrolysis has been modified to include the char volatilization as a significant process at high temperature. According to Barneto et al. [13], for lignocellulosic materials with low lignin content (i.e. pulps), at temperatures higher than 370 °C the main mass loss is related to the volatilization of char that remains in thermobalance.

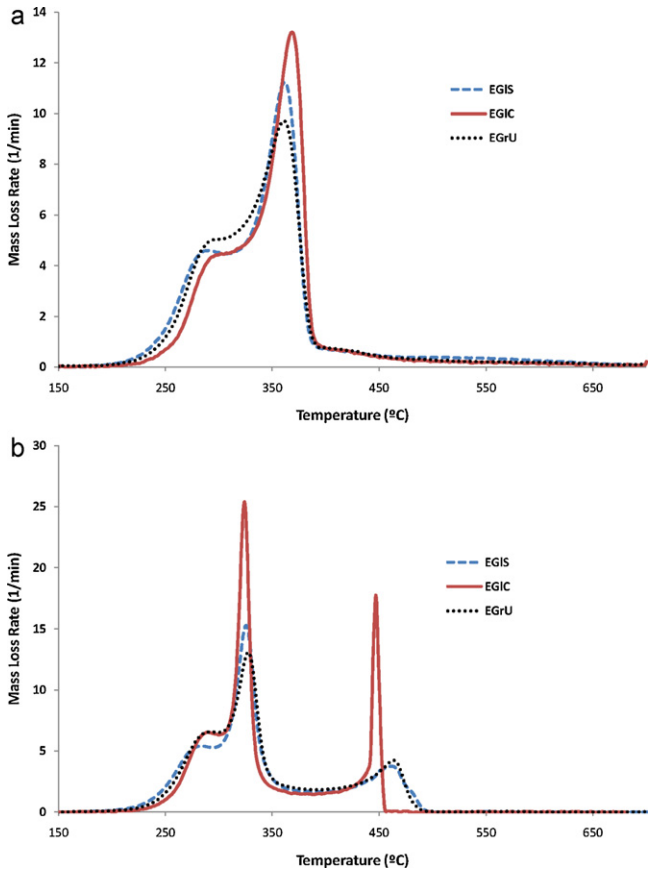

Fig. 3. Thermal degradation behavior of three eucalyptus woods, under nitrogen atmosphere at 10 °C/min (a), and under air atmosphere (b). EGlC is *E. Globulus* from Chile, EGrU is *E. Grandis* from Uruguay, and EGlS is *E. Globulus* from Spain.

The oxidative environment improves the thermal degradation of eucalyptus wood, shifting the cellulosic maximum toward low temperature, and significantly increasing the highest mass loss rate (see Table 3). Under conditions of the thermogravimetric analysis, this process can be interpreted as two consecutive stages. The first stage is a volatilization similar to pyrolysis and the second stage is the result of the char oxidation. This secondary peak can change its shape and position when the heating rate is sufficiently high to produce char ignition (see Fig. 3b). *EGlC* shows the highest thermal degradability, reaching the highest mass loss rates in both atmospheres (see Table 3). Under nitrogen environment their highest mass loss rate is 18% and 36% higher than that obtained for *EGlS* and *EGrU*, respectively. Under air environment these differences go up to 66% and 94%.

Taking into consideration that extractives composition depends on the extraction time and the applied solvent [33], we used an intensive Soxhlet extraction step with a blend of polar and non-polar solvents (ethanol and benzene) during six hours. As extraction does not alter the decomposition pathway of polysaccharides and lignin [33], we can obtain the extractives influence on wood degradation comparing actual and extracted wood samples. According to the results obtained we observed that extractives volatize in a broad temperature interval, between 150 °C and 350 °C, overlapping the degradation of hemicellulose, cellulose and lignin. Moreover, extractives volatilization produces char in a greater proportion than other wood components. This char is

Table 3
Thermal degradation parameters of three eucalyptus woods. Characteristic parameters for the cellulose volatilization peak.

Eucalyptus wood	Pyrolysis		Combustion	
	[a] T_{max} (°C)	[b] v_{max} min^{-1})	T_{max} (°C)	v_{max} (min^{-1})
E. Globulus Chile	368	13.2	324	25.4
E. Globulus Spain	361	11.2	325	15.3
E. Grandis Uruguay	361	9.7	327	13.1

[a] T_{max} the temperature at highest mass loss rate.
[b] v_{max} is the highest mass loss rate.

oxidized in a temperature interval similar to that measured for hemicellulose and cellulose.

As it was expected, with an increasing heating rate the DTG curves are shifted toward higher temperature without significant changes in shape (see Fig. 4a). In this sense, as an example, Table 4 shows the evolution of the highest mass loss rate (v_{max}), and the temperature at highest mass loss rate (T_{max}) when the heating rate increases from 5 to 15 °C/min. In this case, within this heating rates interval, there is a lineal relation between the highest mass loss rate of cellulose volatilization and the heating rate.

Modeling of thermogravimetric curves on the basis of pseudo-components: hemicellulose (H), crystalline cellulose (C_1), amorphous cellulose (C_2), lignin (L) and extractives (E), can explain the thermal degradation of wood. As an example, Table 5 shows the kinetic parameters obtained for the thermal degradation of EGrU wood, under inert and oxidative environments. Likewise,

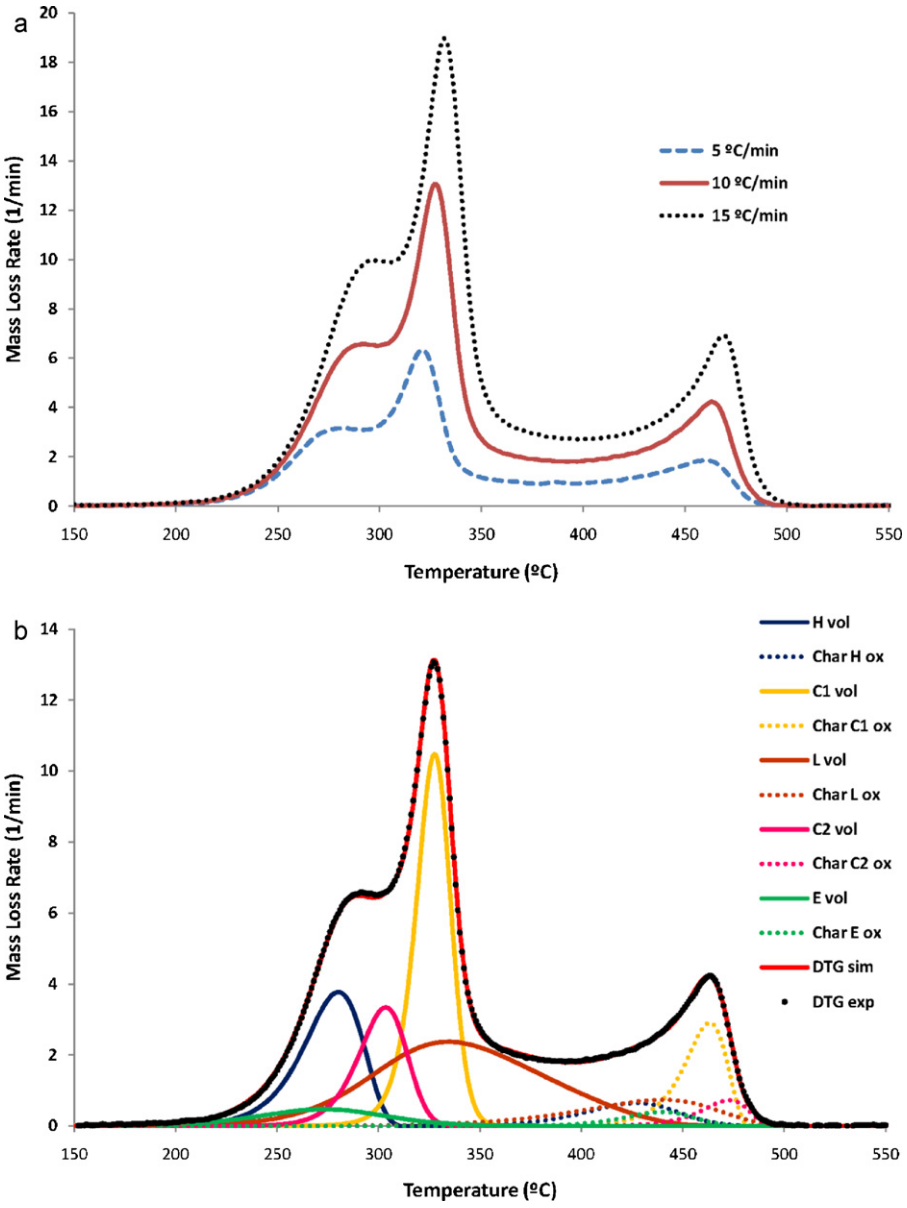

Fig. 4. EGrU wood: (a) effect of the heating rate on the thermal degradation path, and (b) comparison between the experimental and simulated DTG curves (behavior of individual pseudo-components under air atmosphere) at 10 °C/min.

Table 4
Heating rate effect on the thermal degradation of *E. Grandis* wood. Characteristic parameters for the cellulose volatilization peak.

Heating rate (°C/min)	Pyrolysis		Combustion	
	[a]T_{max} (°C)	[b]v_{max} (min^{-1})	T_{max} (°C)	v_{max} (min^{-1})
5	349	4.90	321	6.33
10	361	9.71	327	13.10
15	365	13.70	332	19.01

[a] T_{max} the temperature at highest mass loss rate.
[b] v_{max} is the highest mass loss rate.

Table 5
Kinetic parameters obtained from modeling of the thermal degradation of EGrU wood under oxidative environment.

	Oxidative atmosphere				
	Ln k_o (s^{-1})	E_{act} (kJ/mol)	n	m	V_∞ (%)
H volatilization	13.9 ± 0.1	84 ± 1	0.81 ± 0.01	0.53 ± 0.01	14.3 ± 0.9
C_1 volatilization	33.83 ± 0.01	187 ± 1	1.12 ± 0.03	0.62 ± 0.04	23 ± 2
C_2 volatilization	35.69 ± 0.01	191 ± 1	1.09 ± 0.04	0.27 ± 0.02	10 ± 2
L volatilization	7.04 ± 0.02	61 ± 2	2.83 ± 0.01	0.48 ± 0.01	24.7 ± 0.2
E volatilization	15.09 ± 0.04	92 ± 2	1.48 ± 0.02	0.05 ± 0.01	3.8 ± 0.2
Char *H* oxidation	19.55	142 ± 1	1.08 ± 0.01	0.28 ± 0.01	3.8 ± 0.4
Char C_1 oxidation	19.55	144 ± 2	0.7 ± 0.3	0.7 ± 0.1	8.0 ± 0.7
Char C_2 oxidation	19.55	147 ± 1	0.7 ± 0.1	0.7 ± 0.1	2.2 ± 0.2
Char *L* oxidation	19.55	147 ± 1	1.0 ± 0.1	0.03 ± 0.01	6.4 ± 0.2
Char *E* oxidation	19.55	142 ± 3	0.98 ± 0.04	0.49 ± 0.02	1.8 ± 0.4
Variation coefficient (%)			0.93 ± 0.12		

Table 6
Eucalyptus woods compositions obtained by thermogravimetric analysis.

	H (wt%)	C_1 (wt%)	C_2 (wt%)	*L* (wt%)	Benzene- Ethanol Extractives (wt%)	Cellulose crystallinity (%)	*m*
EGrU wood	18.1	31	12.2	31.1	5.6	71.8	0.62
EGlS wood	21.5	33	11.8	26.2	5.5	73.7	0.84
EGlC wood	20.3	37	13.0	24.0	5.1	74.0	1.10

Fig. 4b compares the experimental and simulated DTG curves and shows the behavior of individual pseudo-components under air atmosphere. The parameters obtained from the fitting process are coherent with chemical composition, crystallinity and kinetic data reported by other authors. Table 6 compares the thermogravimetric composition obtained for studied woods. As it can be seen, the data coincides with the results obtained from the chemical analysis.

On the other hand, the simulation of thermogravimetric analysis gives new information about the analyzed sample: it provides the amorphous cellulose content allowing calculating the cellulose crystallinity as the quotient between the crystalline cellulose content and the global cellulose content, and provides a parameter (the nucleation order, *m*) related to the crystalline cellulose volatilization. Previously cited, *EGlC* produces a cellulosic peak sharper than *EGlS* and *EGrU* (see Fig. 3b). From a kinetic point of view, the peak width is basically related to the reaction order and nucleation order of the crystalline cellulose volatilization. Since the reaction order of this process has similar values for all analyzed woods, the width and the height of cellulosic peaks are directly related with the nucleation order (*m*). Table 6 shows that *EGlC* has the highest value of *m*, being followed by *EGlS* and *EGrU*. A sharp crystalline cellulosic peak, or a high nucleation order, shows that volatilization occurs in a small temperature interval. In our opinion this circumstance is caused by a more crystalline microfibril, that is, with a cleaner and more ordered surface. This fact agrees with an *EGlC* wood with the lowest content in lignin.

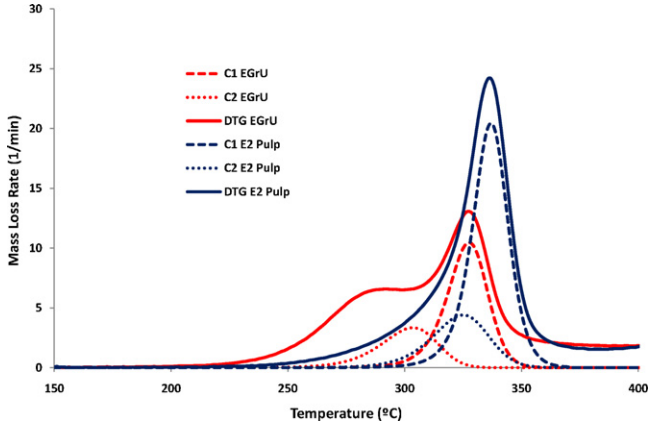

Fig. 5. Comparison between the thermal degradation profiles of EGrU wood and its crude pulp (E2) at 10 °C/min. Changes in cellulosic pseudo-components C_1 (crystalline) and C_2 (amorphous).

3.2. Pulping of eucalyptus wood. Crude pulp characterization

Compositions of crude pulp (E2) and wood (see Tables 1 and 7) coincide with a pulping yield close to 57% and a lignin removal close to 96%. As it was expected, glucan content increases, lignin content diminishes and hemicellulose fraction modifies its composition because galacturonic, glucuronic and acetyl groups present in hemicellulosic fraction of the eucalyptus wood are hydrolyzed by the alkaline environment of the digester.

Pulping increases crystallinity because lignin and hemicellulose removals favor the junction of adjacent elementary microfibrils, promoting the aggregation of crystalline domains [34,35]. As it can be seen in Table 2, crude pulps crystallinity range between 57.1% (for *EGrU*) and 62.5% (for *EGlC*), being their equatorial dimension B_{200} almost two times greater than that measured in woods. Pulp crystallinity is related with wood crystallinity. The more crystalline the wood is (*EGlC*) the more crystalline is the pulp produced.

Table 7
HPLC composition of several pulps obtained from *E. Grandis* wood: E2 crude pulp, E3 oxygen delignified pulp, E4 first chlorine dioxide stage pulp, E5 peroxide stage pulp, E6 second chlorine dioxide stage pulp (dry basis).

	E2 Pulp (wt%)	E3 Pulp (wt%)	E4 Pulp (wt%)	E5 Pulp (wt%)	E6 Pulp (wt%)
Glucan	72.9 ± 0.1	75 ± 1	75.9 ± 0.2	76.2 ± 0.1	75.2 ± 0.2
Xylan	20.3 ± 0.8	19 ± 2	19.8 ± 0.6	19.6 ± 0.6	19.8 ± 0.6
Arabinan	0.06 ± 0.02	0.04 ± 0.06	0.05 ± 0.01	0.06 ± 0.03	0.06 ± 0.02
Galacturonic acid	0.12 ± 0.04	0.11 ± 0.04	0.13 ± 0.02	0.12 ± 0.03	0.12 ± 0.01
Glucuronic acid	0.35 ± 0.01	0.34 ± 0.06	0.30 ± 0.06	0.30 ± 0.01	0.35 ± 0.01
Mannan	1.0 ± 0.1	0.96 ± 0.02	1.0 ± 0.1	0.9 ± 0.1	0.96 ± 0.08
Rhamnose	0.25 ± 0.02	0.2 ± 0.2	0.21 ± 0.01	0.28 ± 0.08	0.27 ± 0.04
Galactan	0.4 ± 0.1	0.5 ± 0.2	0.27 ± 0.06	0.4 ± 0.1	0.38 ± 0.05
Acetyl group	0.02 ± 0.01	0.02 ± 0.01	nd	nd	nd
Klason lignin	2.2 ± 0.7	1.1 ± 0.3	0.98 ± 0.03	0.9 ± 0.1	0.7 ± 0.3

As cellulose is the only crystalline component in both woods and pulps, the crystallinity measure is an indirect measure of crystalline cellulose content. However, crystalline cellulose does not explain the total cellulose content (see Tables 1 and 2). For example for *EGrU* wood the cellulose content is 43.46 wt%, but its crystalline cellulose content is 31.2 wt%. The same conclusion is obtained from their crude pulps. In this case, the cellulose content is 72.89 wt%, but the crystalline cellulose is 57.1 wt%.

Differences between crystalline and total cellulose contents support wood and pulp models which contain amorphous cellulose as pseudo-component. Fig. 5 compares the volatilization of EGrU wood to its crude pulp (E2), showing the degradation profiles of cellulosic pseudo-components (C_1 and C_2). Table 8 shows the kinetic parameters of the pseudo-components degradation in crude pulp obtained from *EGrU* wood. Table 9 shows the composition of several pulps obtained from TG analysis. As it can be seen, the composition of crude pulp (E2) obtained from the thermogravimetric analysis coincides with that obtained from HPLC (see Tables 7 and 9). The main difference is in lignin content because chemical and thermogravimetric analyses have different principles. Whereas klason lignin is acid insoluble lignin (a part of total lignin), pseudo-component lignin (L) includes lignin and other substances which degrade in the same temperature interval. Therefore, klason lignin content in crude pulp (2.17 wt%) is expected to be lower than pseudo-component lignin content (5.1 wt%). In any case, in the studied pulps, it is observed that both measures are related.

From a thermogravimetric point of view, pulping has two effects: it slightly shifts the thermal degradation toward high temperature, and significantly changes the shape of DTG curve. The first effect is related to the washing of wood which removes salts that affect the temperature of cellulose volatilization. The second effect is provoked by significant changes in composition: the removal of hemicellulose makes the shoulder to almost disappear at low temperature, and a greater content of cellulose in pulp makes the cellulosic peak comparatively more important in pulp than in wood. However, despite of these changes, which significantly increase pulp crystallinity (see Tables 6 and 7), the cellulose crystallinity and the nucleation order of crystalline cellulose volatilization increase only slightly by pulping. For example, for *EGrU* the cellulose crystallinity in wood is 71.8% and in its crude pulp is 75.3%. Moreover, for the same samples, the nucleation order for crystalline cellulose volatilization only increases from 0.62 to 0.74. At this point it is necessary to remember that the lignin content is much greater in wood than in pulp.

These data could be explained if it is accepted that pulping removes lignin and hemicellulose but it slightly affects the cellulosic microfibril. The increase of cellulose crystallinity from 71.8% to 75.3% can be explained in two ways: the loss of amorphous cellulose that remains between crystallites in microfibril, or the change from amorphous to crystalline of a part of the superficial cellulose. This last explanation is more acceptable in a pulping context. The core of microfibril is crystalline, but its surface contains crystalline and disordered (amorphous from its thermogravimetric behavior)

Table 8
Kinetic parameters for pseudo-components in crude pulp obtained from EGrU wood.

	Oxidative atmosphere				
	Ln k_o (s^{-1})	E_{act} (kJ/mol)	n	m	V_∞ (%)
H volatilization	14.1	92	0.80	0.25	14.9
C_1 volatilization	34.8	194	1.24	0.74	41.2
C_2 volatilization	34.1	190	1.15	0.37	13.5
L volatilization	6.9	57	1.10	1.06	4.0
Char H oxidation	19.55	137	1.20	0.01	8.0
Char C_1 oxidation	19.55	129	1.16	1.63	12.3
Char C_2 oxidation	19.55	130	1.01	1.59	4.1
Char L oxidation	19.55	143	0.93	1.23	1.1
Variation coefficient (%)			0.53 ± 0.09		

Table 9
Pulps from EGrU wood. Composition based on pseudo-components.

	H (wt%)	C_1 (wt%)	C_2 (wt%)	L (wt%)	Cellulose crystallinity (%)	m
E2 pulp	22.9	53.5	17.6	5.1	75.3	0.74
E3 pulp	21.2	58.4	17.2	2.2	77.2	0.86
E4 pulp	21.4	58.9	16.9	2.3	77.7	0.94
E5 pulp	21.5	59.2	16.9	1.7	77.8	1.04
E6 pulp	20.8	58.8	16.9	3.2	77.7	0.69

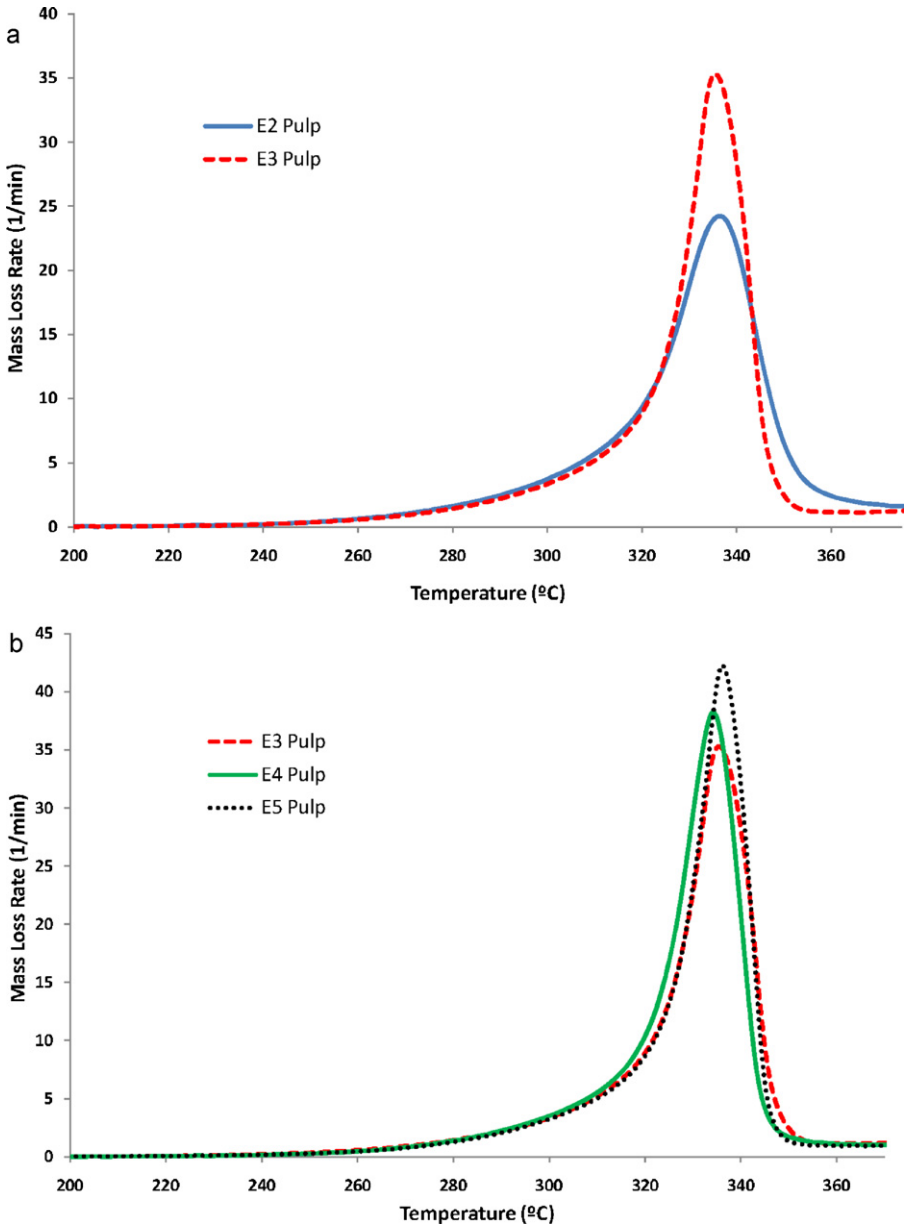

Fig. 6. Thermogravimetric monitoring of pulps at 10 °C/min: (a) comparison between crude pulp (E2) and oxygen delignified pulp (E3), (b) comparison between oxygen delignified pulp (E3), dioxide chlorine treated pulp (E4) and peroxide treated pulp (E5).

cellulose. Superficial cellulose is disordered in the zones that bond other substances like hemicellulose or lignin. As pulping breaks these bonds, the microfibril surface recovers crystallinity. However, since the increase in cellulose crystallinity is small, it must be accepted that cellulose microfibril remains minimally altered by pulping. This explanation coincides with a slight increase in nucleation order (m) from 0.62 in wood to 0.74 in crude pulp. As previously commented, an increase in m is caused by a cleaner and more ordered microfibril surface.

Thus, the thermogravimetric analysis describes pulping as a process that basically degrades bulk amorphous hemicellulose and lignin located among cellulose microfibrils, increasing the crystallinity of pulp. However, this process hardly modifies the cellulosic microfibrils, maintaining or slightly increasing the cellulose crystallinity. In the course of pulping the microfibril aggregation could be important which explains the increases of their equatorial dimensions by almost double.

3.3. Delignification and bleaching

In the pulp mill the crude pulp (E2) is consecutively oxygen delignified (E3) and bleached according to D–P–D (chlorine dioxide–peroxide–chlorine dioxide) sequence, which produces E4, E5 and E6 pulps, respectively. In order to study the effects of these

Table 10
Crude pulp characteristics (E2). Effect of the oxygen delignification (E3), first chlorine dioxide step (E4), hydrogen peroxide treatment (E5) and second chlorine dioxide step (E6).

	Kappa number	Brightness (%)	Viscosity (mL/g)
E2 pulp	16.0	33	1110
E3 pulp	9.5	52	960
E4 pulp	2.1	77	905
E5 pulp	1.7	86	880
E6 pulp	1.5	88	865

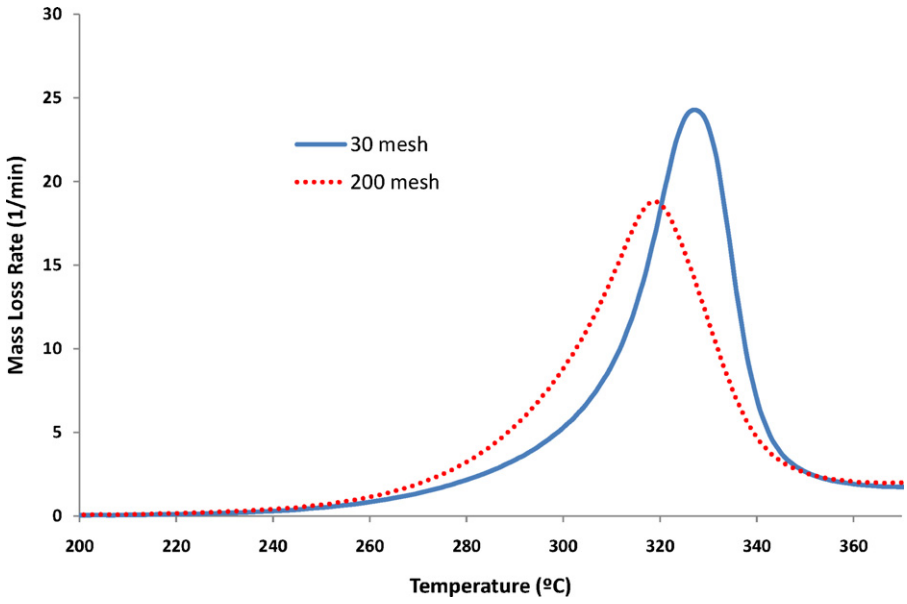

Fig. 7. Effect of the fibre size on the thermal degradation path of pulps under oxidative environment at 10 °C/min.

Table 11
Pulp crystallinity and equatorial dimension obtained from X-ray diffraction.

	Pulp crystallinity XRD (%)	Equatorial dimension B_{200} (nm)
Global pulp	62.5	4.1
LSPF	62.6	4.1
MSPF	62.6	4.0
SSPF	60.7	3.8

treatments, pulps were analyzed using X-ray diffraction, HPLC and TGA. Tables 7 and 9 show compositions based on sugar monomers and pseudo-components, respectively. Likewise Fig. 6 compares the thermal degradation profiles of pulps. Table 10 shows the effects of these treatments on kappa number, brightness and viscosity. As it can be seen, the bleaching process diminishes kappa number and viscosity but increases brightness. These changes are asymptotic, that is, the next treatment has a smaller effect than the previous one.

Table 7 shows that the main chemical changes occur during oxygen delignification; increased glucan content from 72.89 wt% to 74.94 wt% and, at the same time, significantly decreased lignin content from 2.17 wt% to 1.09 wt% were obtained. Along with pulping, this is the most effective process for lignin removal. Thermogravimetric analyses confirm this results, showing that the lignin pseudo-component content diminishes from 5.1 wt% to 2.2 wt%. Likewise Fig. 6a shows that oxygen delignification has a significant effect on the thermal degradation behavior of pulp, making cellulosic peak narrower and higher than in crude pulp. As residual lignin thermally degrades between 340 and 360 °C, its removal causes E3 pulp peak to become narrower than E2 pulp peak. This change has a consequence on kinetic parameters of cellulose volatilization: the reaction order diminishes from 1.24 to 1.00. On the other hand, according to the thermogravimetric simulation, the cellulosic peak in E3 pulp is higher than in E2 pulp because of two reasons: (i) the crystalline cellulose content increases from 53.5 wt% to 58.4 wt%, and (ii) the microfibril surface is cleaner than in crude pulp (the nucleation order increases from 0.74 to 0.86). Consequently, both the lignin removal and a more crystalline microfibril surface (cellulose crystallinity increased from 75.3% to 77.2%) explain the increase in the highest mass loss rate from 22.8 min^{-1} in E2 to 35.2 min^{-1} in E3.

During the bleaching stages the chemical composition of pulps hardly changes. As it occurs during oxygen delignification, there is a slight increase in glucan content accompanied by a slight decrease in lignin content. The same conclusions are achieved from TGA. The crystalline cellulose content increases slightly but the cellulose crystallinity remains practically constant (between 77.7% and 77.8%). However, the bleaching process has an effect on the thermal degradation behavior of pulps. Fig. 6b shows that both chlorine dioxide and peroxide treatments make the cellulosic peaks sharper,

Table 12
Chemical composition of pulps with different sizes of fibers (dry basis).

	Glucan (wt%)	Xylan (wt%)	Arabinan (wt%)	Rhamnose (wt%)	Klason Lignin (wt%)
Global Pulp	78.1 ± 0.2	18.6 ± 0.6	0.18 ± 0.02	0.12 ± 0.02	2.2 ± 0.2
LSPF	79.6 ± 0.1	17.9 ± 0.8	0.18 ± 0.01	0.11 ± 0.04	1.9 ± 0.3
MSPF	79.5 ± 0.2	19.1 ± 0.4	0.20 ± 0.03	0.14 ± 0.04	2.2 ± 0.3
SSPF	75.5 ± 0.4	19.7 ± 0.3	0.19 ± 0.02	0.13 ± 0.01	2.8 ± 0.1

Table 13
Pulps compositions based on pseudo-components.

	H (wt%)	C_1 (wt%) (3)	C_2 (wt%) (4)	*L* (wt%) (5)	Nucleation order of C_1 volatilization (m)	Cellulose crystallinity (%)
Global Pulp	17.3	61.7	14.0	5.8	0.52	81.6
LSPF	16.2	63.9	13.7	5.5	0.66	82.3
MSPF	17.2	62.1	13.8	5.6	0.54	81.8
SSPF	18.1	60.6	13.8	5.8	0.48	81.5

increasing both the nucleation order (see Table 9) and the highest mass loss rate, which changes from 35.2 min^{-1} in E3 to 37.3 min^{-1} in E4 (first chlorine dioxide step) and 42.3 min^{-1} in E5 (peroxide step). These facts are coherent with a progressively cleaner microfibril surface.

3.4. Influence of the fibre size in the pulp properties

In order to better understanding the influence of pulping on fibers with different length, a sample of crude pulp (global) from *EGlC* was separated in three fractions according to the fibre sizes. Using three consecutive filtration steps, 55.7 wt% of the initial pulp was retained by a 30 mesh filter (large size pulp fibre, *LSPF*), 23.0 wt% by a 50 mesh filter (medium size pulp fibre, *MSPF*), and 12.7 wt% by a 200 mesh filter (short size pulp fibre, *SSPF*). The difference to 100% (8.6 wt%), are fines which pass through the 200 mesh filter.

As we can see in Table 11, pulp crystallinity measured by X-ray diffraction corresponds to the crystalline cellulose content calculated by thermogravimetric analysis. On the other hand, the chemical composition coincides with the composition based on pseudo-components (see Tables 12 and 13). These data confirm that fibers with different sizes show different compositions and structural properties. When fibre size increases, lignin and hemicellulose contents diminish and glucan content increases. This fact has an influence in pulp and cellulose crystallinity, which achieve the highest values in *LSPF*. On the contrary, *SSPF* has the lowest crystallinity and equatorial dimension (3.8 nm).

As it was expected, the thermal degradation profile is also affected by fibre size. According to Fig. 7, the fibre with largest size (*LSFP*) volatilizes at higher temperature with the highest mass loss rate. On the contrary, the fibre with smallest size (*SSFP*) (with more hemicellulose and lignin) yields a broad peak at lower temperature. The nucleation order of crystalline cellulose volatilization in *LSFP* is 0.66, but in *SSFP* is 0.48. A higher nucleation order is associated with a cleaner and more crystalline cellulose microfibril.

4. Conclusions

Thermogravimetric analyses can be used to monitor the pulping process in a pulp mill. The chemical changes that wood and pulps undergo influence their thermal degradation behavior. As a basic rule, as pulping and bleaching progress, the volatilization of crystalline cellulose occurs in a narrower temperature interval. The simulation of thermogravimetric data allows obtaining significant information about the thermal degradation of the main components of the samples.

There are significant differences between chemical compositions and thermal degradations in eucalyptus wood from different species or geographical origins. In analyzed samples, *E. Globulus* wood from Chile, with the lowest lignin content, has the highest thermal degradability, showing as twice as the mass loss rate shown by *E. Grandis* from Uruguay under air environment.

With the modeling of the thermogravimetric analysis of woods, it is possible to obtain their composition on the basis of five pseudo-components which include crystalline and amorphous celluloses. From this approximation, wood cellulose crystallinity was also calculated, being greatest in *E. Globulus* from Chile. The obtained data coincide with that reported by X-ray diffraction and chemical analysis.

Pulping mainly removes bulk hemicellulose and lignin, but has small effect on these substances when they are linked to cellulose microfibril. This is why pulp crystallinity is significantly greater than wood crystallinity (i.e. for *EGrU* is 57.1% in crude pulp and 31.2% in wood), but cellulose crystallinity hardly changes (i.e. for *EGrU* is 75.3% in crude pulp and 71.8% in wood). A slight increase in cellulose crystallinity is the consequence of slight and incomplete removal of substances linked to microfibril. In this case, the breakages of bonds cause superficial cellulose to regain order and crystallinity, increasing the whole microfibril crystallinity. In this process adjacent microfibrils result linked, increasing the equatorial dimension of microfibril. This interpretation is coherent with a slight increase in the nucleation order of crystalline cellulose volatilization.

Oxygen delignification and the bleaching process based on chlorine dioxide and hydrogen peroxide diminishes lignin content in pulp and modifies its thermal degradation profile, sharpening the peak associated to crystalline cellulose volatilization. This fact, accompanied by an increase in the nucleation order, is the consequence of a cellulosic microfibril surface that is progressively cleaner, more ordered and, consequently, more crystalline. This conclusion is supported by a reduction in the kappa number and an increase in brightness.

The fibre size has an influence on the composition and thermal behavior of pulp. The pulp with the greatest fibre size has the highest content in cellulose and the lowest content in hemicellulose and lignin. At the same time, this pulp shows the highest mass loss rate during crystalline cellulose volatilization (peak sharper in DTG curve).

Acknowledgements

This work has been promoted by the Agreement between the ENCE group and the University of Huelva. ENCE mill at Huelva (Spain) is gratefully acknowledged for supplying the woods and pulps.

References

[1] Y. Nishiyama, U.J. Kim, D.Y. Kim, K.S. Katsumata, R.P. May, P. Langan, Periodic disorder along ramie cellulose microfibrils, Biomacromolecules 4 (2003) 1013–1017.
[2] A.C. O'Sullivan, Cellulose: the structure slowly unravels, Cellulose 4 (1997) 173–206.
[3] D. Fengel, Ideas on ultrastructural organisation of cell-wall components, J. Polym. Sci.: Part C 36 (1971) 383–392.
[4] K. Wickholm, P.T. Larsson, T. Iversen, Assignment of non-crystalline forms in cellulose 1 by CP/MAS ^{13}C NMR spectroscopy, Carbohydr. Res. 312 (1998) 123–129.
[5] A.P. Heiner, L. Kuutti, O. Teleman, Carbohydr. Res. 306 (1998) 205–220.
[6] CEPI, Key Statistics, European Pulp and Paper Industry, 2009, http://www.cepi.org/Content/Default.asp?PageID=4. Accessed 12/14/2010.
[7] E. Sjostrom, Wood Chemistry: Fundamentals and Applications, Academic Press, New York, 1981.
[8] N. Hartler, Extended delignification in kraft cooking – a new concept, Sven. Papperstidn. 81 (1978) 483–484.
[9] S. Norden, A. Teder, Modified kraft processes for softwood bleached-grade pulp, Tappi J. 62 (1979) 49–51.
[10] T. Blain, Anthraquinone pulping: fifteen years later, Tappi J. 76 (1993) 137–146.
[11] O. Faix, E. Jakab, F. Till, T. Szekely, Study on low mass thermal degradation products of milled woods lignins by thermogravimetry–mass spectrometry, Wood Sci. Technol. 22 (1988) 323–334.
[12] G. Varhegyi, M.J. Antal, T. Szekely, P. Szabó, Kinetics of the thermal decomposition of cellulose, hemicellulose, and sugar cane bagasse, Energy & Fuels 3 (1989) 329–335.
[13] A.G. Barneto, J. Ariza, J.E. Martín, R. Sánchez, Simulation of the thermogravimetry analysis of three non-wood pulps, Bioresour. Technol. 101 (2010) 3220–3229.
[14] R.J. Evans, T.A. Milne, Molecular characterization of the pyrolysis of biomass, 1. Fundamentals, Energy & Fuels 2 (1987) 123–137.
[15] E. Meszaros, E. Jakab, G. Varhegyi, P. Tovari, Thermogravimetry/mass spectrometry analysis of energy crops, J. Thermal Anal. Calorim. 88 (2007) 477–482.
[16] M.B. Roncero, J.F. Colom, T. Vidal, Influencia de los tratamientos enzimáticos con xilanasas en la composición de hidratos de carbono de pastas para papel, Afinidad 60 (2003) 8–15.
[17] C. Di Blasi, M. Lanzetta, Intrinsic kinetics of isothermal xylan degradation in inert atmosphere, J. Anal. Appl. Pyrol. 40 (1997) 287–303.
[18] M. Antal, G. Varhegyi, E. Jakab, Cellulose pyrolysis kinetics: revisited, Ind. Eng. Chem. Res. 37 (1998) 1267–1275.

[19] R. Capart, L. Khezami, A. Burnham, Assessment of various kinetic models for the pyrolysis of a microgranular cellulose, Thermochim. Acta 417 (2004) 79–89.
[20] J. Jauhiainen, J.A. Conesa, R. Font, I. Martin-Gullon, Kinetics of the pyrolysis and combustion of olive solid waste, J. Anal. Appl. Pyrolysis 72 (2004) 9–15.
[21] V. Mamleev, S. Bourbigot, M. Le Bras, J. Yvon, J. Lefebvre, Model-free method for evaluation of activation energies in modulated thermogravimetry and analysis of cellulose decomposition, J. Chem. Eng. Sci. 61 (2006) 1272–1288.
[22] A.G. Barneto, J. Ariza, J.E. Martin, L. Jiménez, Use of autocatalytic kinetics to obtain composition of lignocellulosic materials, Bioresour. Technol. 100 (2009) 3963–3973.
[23] J.J. Orfao, F. Antunes, J.L. Figueiredo, Pyrolysis kinetics of lignocellulosic materials three-component reactions model, Fuel 78 (1999) 349–358.
[24] E. Meszaros, G. Varhegyi, E. Jakab, B. Marosvölgyi, Thermogravimetric and reaction kinetic analysis of biomass samples from an energy plantation, Energy & Fuels 18 (2004) 497–507.
[25] S.S. Alves, J.L. Figueiredo, Pyrolysis kinetics of lignocellulosic materials by multistage isothermal thermogravimetry, J. Anal. Appl. Pyrolysis 13 (1988) 123–134.
[26] M.G. Grønli, G. Varhegyi, C. Di, Blassi Thermogravimetric analysis and devolatization kinetics of wood, Ind. Eng. Chem. Res. 41 (2002) 4201–4208.
[27] O. Senneca, Kinetics of pyrolysis, combustion and gasification of three biomass fuels, Fuel Process. Technol. 88 (2007) 87–97.
[28] P. Naredi, S.V. Pisupati, Interpretation of char reactivity profiles obtained using a thermogravimetric analyzer, Energy & Fuels 22 (2008) 317–320.
[29] E.G. Prout, F.C. Tompkins, The thermal decomposition of potassium permanganate, Trans. Faraday Soc. 40 (1944) 488–498.
[30] E.G. Prout, F.C. Tompkins, The thermal decomposition of silver permanganate, Trans. Faraday Soc. 42 (1946) 468–472.
[31] A.K. Burnham, R.L. Braun, T.T. Coburn, E.I. Sandvik, D.J. Curry, B.J. Schmidt, R.A. Noble, An appropriate kinetic model for well-preserved algal kerogens, Energy & Fuels 10 (1996) 49–59.
[32] S. Andersson, R. Serimaa, T. Paakari, P. Saranpää, E. Pesonen, Crystallinity of wood and the size of cellulose crystallites in Norway spruce (Picea abies), J. Wood Sci. 49 (2003) 531–537.
[33] E. Meszaros, E. Jakab, G. Varhegyi, TG/MS Py–GC/MS and THM-GC/MS study of the composition and thermal behavior of extractive components of *Robinia pseudoacacia*, J. Anal. Appl. Pyrolysis 79 (2007) 61–70.
[34] M.Y. Ioelovitch, A.D. Tupureine, G.P. Veveris, Study on the cellulose cocrystallinization during it isolation from plant raw materials, Khim Drevesiny 4 (1991) 27–33.
[35] E.L. Hult, P. Larsson, T. Iversen, A CP/MAS 13C NMR study of supermolecular changes in the cellulose and hemicellulose structure during kraft pulping, Nordic Pulp Paper Res. J. 16 (2001) 33–39.